Digital Pacer Detection in Diagnostic Grade ECG

Mohammed Shoaib
Department of Electrical Engineering
Princeton University NJ 08544
Email: mshoaib@princeton.edu

Harinath Garudadri
Qualcomm Inc
5775 Morehouse Dr., San Diego CA 92122
Email: hgarudad@qualcomm.com

***Abstract*—Pulses from a cardiac pacemaker appear as extremely narrow and low- amplitude spikes in an ECG. These get misinterpreted for R-peaks by QRS detectors, leading to subsequent faulty analysis of several algorithms which rely on beat-segmentation. Detection of the pacer pulses, thus, necessitates sampling the ECG signal at high data rates of 4-16 kHz. In a wireless body sensor network, transmission of this high-bandwidth data to a processing gateway, for pacer detection, is extremely power consuming. In this paper, we describe a compressed sensing approach, which enables reliable detection of AAMI/EC11 specified pacer pulses using ECG data rates of 50-100 sps, an order of magnitude smaller than those used in typical detection algorithms in the literature.**

I. Introduction

Wireless sensor networks enable observation and retrieval of information from the ambient in a versatile manner. The coalescence of self-coordinating micro-sensor nodes has enabled low-power, ultra-mobile body-sensor-networks (BSN) [1], [2]. Fig. 1 illustrates a BSN, where wireless sensors are used to sense vital signs and communicate them among each other and to an aggregator, such as a personal-data-assistant (PDA) or a cell phone. These devices facilitate inter-node connectivity as well as a communication interface to a wide-area healthcare network involving a physician and a centralized server [3]. Sensor nodes and computation

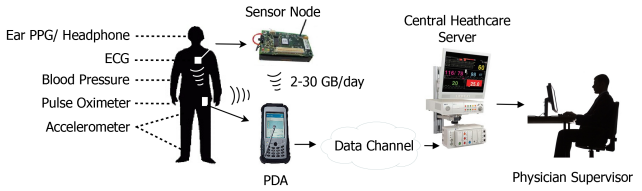

Fig. 1. A body sensor network comprises of wireless sensor nodes which communicate among themselves and with an aggregator.

platforms in BSNs, necessitate energy efficient communication of data. Continuous and routine monitoring of physiological signals, such as the electrocardiogram (ECG) and the electroencephalogram (EEG) leads to a deluge of information. A transceiver on a BSN sensor node, typically requires an aggregate data rate of 5-50 kbps [4] and, thus, for example, continuous transmission of 12-lead ECG of a healthy individual, entails nearly 2.77 GB of raw data per-day [5]. At a sampling rate of 4 kHz, this can reach up to 31 GB. Hence communication techniques which invoke compression and encoding are essential.

In addition to physiological signals, in modern medical systems, artificial signal sources impose further limitations on the network data. Cardiac pacemakers are a typical example. A pacemaker uses an electrical pulse as a stimulation signal to excite the various chambers of the heart. These appear as low-amplitude, short-duration spikes in the ECG signal and their detection is important for accurate beat-detection and classification. The detection of the pacemaker response entails distinction of pacing pulses from the electrical response of the heart. Modern pacemakers generate pulses of 2-5 mV which last for about 0.5-2 ms in an ECG recording. Reliable detection of the pacing pulses, thus necessitates, high sampling rates (4-16 kHz) in order to capture enough energy from the narrow pulses [6], [7]. Several detection schemes are possible with the basic event detection (or sensing) algorithm remaining more or less unchanged, based on high-pass filtering followed by an amplitude threshold [7]. Software based detection systems have been proposed in [8]–[10]. While [8] uses a 32 ksps ECG stream for single-threshold bi-ventricular pacer detection, [9] and [10] uses an adaptive threshold based 2-slope approach for dual chamber pacing. These algorithms, however, have shown to be sensitive to EMG noise and, thus fail to detect narrow pulses with a low SNR [11]. The non-linear filtering approach in [11] and [12] overcomes the SNR problem. The transmission efficiency of these approaches in a body sensor network, however, is limited by the high sampling rate of 8-10 kHz.

978-1-61284-697-2/11/$26.00 ©2011 IEEE

In [13], we presented reliable telemetry for diagnostic grade ECG using compressed sensing (CS) for error resiliency. In this paper, we use CS to reduce the number of measurements required for accurate pacer pulse detection. The specific contributions are as follows:

- We develop a baseline algorithm for threshold pacer detection consisting of a linear high pass filter, correlation filter and a threshold detector. This is a hybrid approach based on [7], [9] and [11].
- We make use of patient data from the MIT-BIH normal sinus rhythm database (NSRDB) [14] and pacer models from the ANSI/AAMI EC11 standard [15] for our analysis, and show that reliable detection of pulses, which last for about 0.5-2 ms, necessitates high sampling rates (f_s) of the order of 4-16 kHz.
- We present a CS based *sub-band reconstruction algorithm* which enables reliable detection of pacer pulses using only about 1% (50-100 sps) of the 4-16 kHz sampled data. Our framework comprises of random sampling from a DCT sub-space and GPSR based reconstruction [16].

The rest of the paper is organized as follows: In Sec. II, we give a brief overview of compressed sensing and the challenges associated with pacer detection. In Sec. III, we describe the baseline algorithm used followed by simulation results showing its performance degradation with sample rate reduction. In Sec. IV, we describe the CS based detection algorithm and present a comparative analysis with the baseline algorithm. Finally, we conclude in Sec. V.

II. Background

ECG signals, acquired using an electrode and wearable wireless sensors, are processed using an analog front end and a digital back end. Fig. 2 shows the possible stages

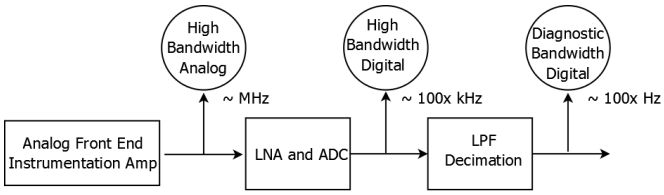

Fig. 2. Pacer detection at three levels of signal acquisition

for pacer detection. Pacemaker pulses in the ECG are high frequency signals, and their detection has traditionally been done in the front-end of electrocardiograph devices, on high bandwidth signals [6]. Some devices use analog circuitry to detect the large signal slew-rates typical of pacemaker pulses. These circuits are, however, inflexible to adapt to varying pacer signal characteristics and are prone to poor specificities [9]. While some other methods use high bandwidth digital signals, the detection of pacer signals using diagnostic grade ECG (sub 1 kHz or ksps sampling rates) for narrow (0.5-2 ms/ 2-5 mV), EC11 specified pulses has not been explored.

The pacer pulse characteristics specified by the ANSI/AAMI standard for diagnostic electrocardiograph devices [15] are shown in Fig. 3 and summarized in Table. I. APulse and TPulse are the amplitude and

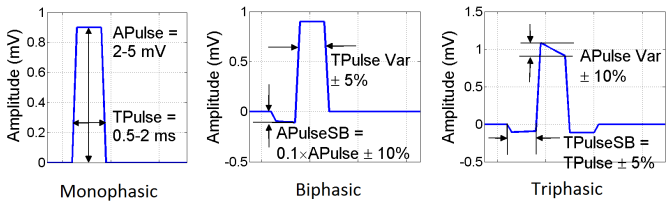

Fig. 3. ANSI/AAMI EC11 pacer pulse definitions: Monophasic, bi-phasic and tri-phasic pulses.

duration of the pacer pulse signals with APulse Var and TPulse Var standing for their percentage variances respectively. APulseSB and TPulseSB are the amplitude and duration of the pacer pulse side-bands in bi- and tri-phasic pulses. As is seen from the table, cardiac

TABLE I
Diagnostic ECG pacer pulse specifications, ANSI/AAMI EC11

Pulse parameter	Specification
Pacing mode	Demand or rate regulated
Excitation mode	Cathode or anode
Excitation phase	Mono-,bi- or triphasic
TPulse ± Var	0.5-2 ms ± 5%
APulse ± Var	2-5 mV ± 10%
TPulseSB ± Var	TPulse ± 5%
APulseSB ± Var	10% APulse ±10 %
Rise and fall times	≤ 100 μs
Average pulsing rate	~ 100/min

pacing can potentially be done in an on-demand or rate regulated manner using anodic or cathodic excitation. In the rest of this paper, we focus on the most common case of pacing with results generalizable to others. We will use a demand pacing mode and cathodic excitation with monophasic pulses. We will use rise and fall times of 100 μs and an average pulse rate of 100 pulses/min.

Compressed Sensing

A new paradigm called compressed (or compressive) sensing (CS) is emerging as an efficient communication approach to networked data in sensor networks [17]. In our CS approach for pacer detection, *priors*, or characteristics typical of the pacer pulse are exploited to enable transmission of *just-enough information* over the air. Following accurate reconstruction, at a centralized

processing interface, a fraction (50-100 sps) of the 4-16 kHz ECG samples are used for reliable pacer-pulse detection.

The theory of CS is based on the principles of uncertainty and the concept of incoherence between two bases. It states that a signal having a sparse representation in one basis can be recovered from a small number of projections onto a second basis that is incoherent with the first. Suppose a signal $\vec{x} \in R^N$ is K sparse in a basis Ψ. This means $\vec{x}$ can be well approximated by a linear combination of a small set of vectors in Ψ, *i.e.*, $\alpha = \sum_{i=1}^{K} b_i \psi_i$, where α is the transformation $\Psi\vec{x}$, b_i is a non-zero scalar, ψ_i is the i^{th} column vector of Ψ, and $K \ll N$. The theory of compressed sensing states that it is possible to use a $M \times N$ measurement matrix Φ, where $M \ll N$, and reconstruct $\vec{x}$ from the measurements,

$$y = \Phi x \tag{1}$$

The advantage of using CS is based upon the fact that the measurement matrix Φ has the lone constraint that it should be incoherent with Ψ and can be a random matrix under the restricted isometry property (RIP) [18], [19]. The reconstruction (or decoding) of the original signal $\vec{x}$ from the measurement matrix is a complex, non-linear convex optimization problem. The under determined set of equations can be eventually solved as,

$$\underset{x}{\operatorname{argmin}} \left[\|y - \Phi x\|^2 + \tau \|\Psi x\|^1 \right] \tag{2}$$

This is the method of gradient projection sparse reconstruction (GPSR), which has been shown to outperform matching pursuit and iterative shrinking algorithms [16].

III. Differential Filter Pacer Detector

In this section, we describe a baseline algorithm for pacer detection. Fig. 4 shows the block diagram of the algorithm.

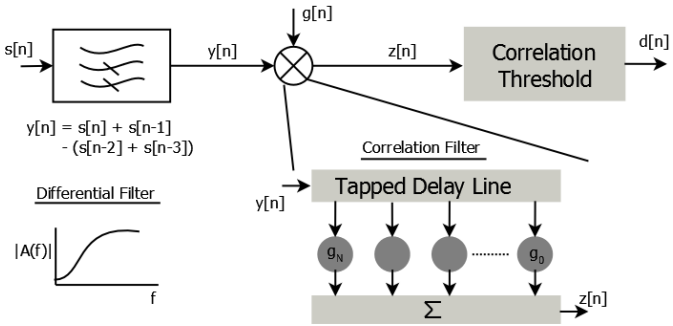

Fig. 4. Pacer pulse detection using thresholding correlation filters.

$s[n]$ is the ECG signal with the pacer pulse. It is high-pass filtered using the pre-processing differential filter, $y[n]$ from [9], which has a frequency response $A(f)$. In the time domain, $y[n]$ is given as,

$$y[n] = s[n] + s[n-1] - (s[n-2] + s[n-3]) \tag{3}$$

The high pass filter produces the ECG free signal $y[n]$ which is then processed using a correlation filter akin to the approach in [7]. The correlation coefficient, $g[n]$ is an ideal pulse signal based on the ANSI/AAMI specifications of Table. I, with the variances TPulse Var and APulse Var set to zero. The correlation filter is implemented using a tapped delay line which eventually leads to the correlation result $z[n]$ given by,

$$z[n] = \left| \sum_{k=-inf}^{inf} \frac{y[n]g[n-k]}{\|g\|.\|y\|} \right| \tag{4}$$

where $\|\cdot\|$ is the second order norm. This is compared with a single-threshold to determine if $s[n]$ contains a pacer signal based on the correlation value $d[n]$.

A. Experimental setup

In this section, we describe the experimental setup to evaluate the baseline detection algorithm and the proposed sub-band CS reconstruction algorithm for pacer detection. We use two different ECG signal sources ($s_{ECG}[n]$) to evaluate our detection algorithms: (1) ECGsyn [20] based synthetic ECG and, (2) Real patient data from the MIT-BIH NSRDB [14]. Furthermore, synthetic EC11 pacer pulses ($p[n]$) with specifications as shown in Table. I are used in an on-demand manner. We generate the pacer signals in Matlab and superimpose them with the ECG from the above two sources to generate a cathode excited, monophasic paced ECG signal with an average pacing rate of 100 pulses/min. We model three noise sources ($w[n]$), similar to those described in [11]. The total paced ECG signal, $s[n]$ from Sec. III is, thus a superposition of these three signals and is given by,

$$s[n] = s_{ECG}[n] + p[n] + w[n] \tag{5}$$

In Eq. (5), the three noise sources used are (1) Baseline wander (BW) due to patient respiration and movement (0.05- Hz), (2) Power Line Interference (PLI) consisting of a 60 Hz sinusoid, and (3) Electromyographic (EMG) noise which is introduced by the muscular activity (AWGN wide-band). Thus, $w[n]$ is given by,

$$w[n] = \beta_{BW} w_{BW}[n] + \beta_{PLI} w_{PLI}[n] + \beta_{EMG} w_{EMG}[n] \tag{6}$$

where, $\beta^2_{BW}, \beta^2_{PLI}, \beta^2_{EMG}$ are the powers of each of the noise sources. These are modulated to scale the SNR of the total signal $s[n]$.

Fig. 5 shows the simulation setup used for the pacer detection experiments in this paper. The noise and pacer models are superimposed with the synthetic (ECGsyn) or real patient data (MIT-BIH, NSRDB) which are then subjected to two detection methods, (1). Differential filter detector, and (2) CS sub-band reconstruction detector.

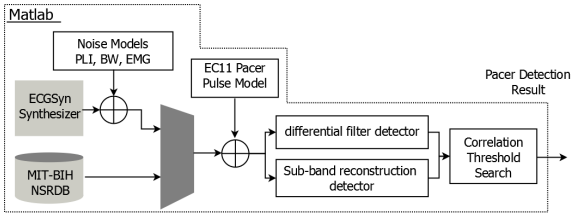

Fig. 5. Simulation setup for evaluation of the pacer detection.

B. Baseline detector performance

In this section we present, evaluation results for the pacer detection algorithm of Sec. III. We evaluated the baseline algorithm on the MIT-BIH NSR database and Fig. 6 shows the scaling of specificity, sensitivity and the accuracy [1] of the detection algorithm with the sampling frequency. We evaluated the algorithm using the up sampled MIT-BIH ECG data at 1, 2, 4, and 8 kHz using a 5 mV pacer pulse of 1 ms duration. The x-axis shows the evaluation on the various patient records and the y-axis shows the scaling of the maximum sum which is the average of the specificity, sensitivity and accuracy values. The maximum sum was chosen as an evaluation metric as the objective of the algorithm was to maximize all three measures (specificity, sensitivity and accuracy) equally.

Fig. 7 shows the performance of the baseline algorithm for Rec#16265 as the amplitude of the pacer pulse and the sampling rate (f_s) is reduced. As is seen from the

[1]Sensitivity = $\frac{T_P}{T_P+F_N}$, Specificity = $\frac{T_N}{T_N+F_P}$ and Accuracy = $\frac{T_P+T_N}{T_P+F_P+T_N+F_N}$ where $T(F)_{N(P)}$ is the number of true (false) negatives (positives). Maximum Sum = (Sensitivity+Specificity+Accuracy)/3

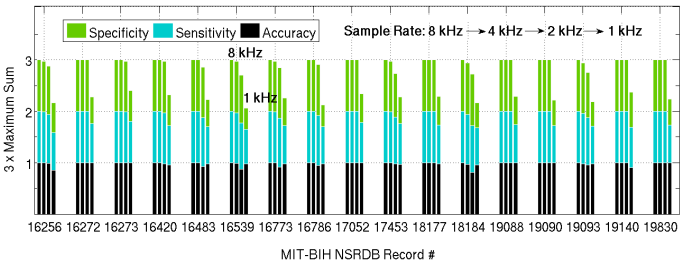

Fig. 6. The performance of the differential detector on the MIT-BIH NSRDB deteriorates with reducing sampling rates. Shown at APulse = 5 mV, TPulse = 1 ms, cathode excited, monophasic pulses.

figure, detection of the pacer becomes more and more difficult as the pacer amplitude and the sampling rate drops. The measurements are made at a constant SNR. The pulse and ECG SNRs are calculated as ,

$$Pulse\ SNR = \beta^2_{p[n]} / \left(\beta^2_{s_{ECG}[n]} + \beta^2_{w[n]}\right) \quad (7)$$

$$ECG\ SNR = \beta^2_{s_{ECG}[n]} / \left(\beta^2_{p[n]} + \beta^2_{w[n]}\right) \quad (8)$$

where, $\beta^2_{p[n]}$, $\beta^2_{w[n]}$, $\beta^2_{s_{ECG}[n]}$ stand for the powers of the pacer, noise and the ECG signal respectively. Fig. 8 shows the scaling of the differential filter detector performance versus the pacer duration and the sampling rate (f_s). The correlation detector also fails at low SNR values and, as is seen from Fig. 9, for acceptable maximum sum in the typical ECG SNR range of 8-20 dB, a sampling rate of 16 kHz or higher is necessary.

IV. CS Sub-Band Reconstruction Algorithm

Reliable pacer detection using differential filtering followed by a correlation threshold requires high sampling rates of the ECG signal of up to16 kHz or more. In this section, we describe a CS-based algorithm for reliable pacer detection using over the air data rates of only about 50-100 sps.

The differential-filtered signal, $d[n]$, has reminiscent ECG energy dominating the 0-50 Hz band co-located with the pacer signal. This is shown in Fig. 10-(A-C).

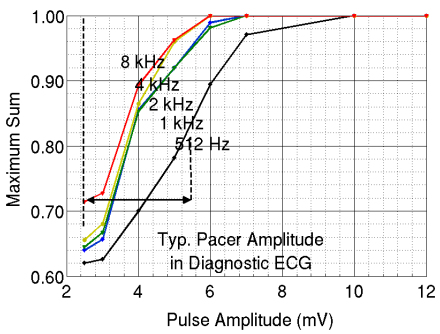

Fig. 7. Max. sum falls with low ampl. pulses and f_s. Shown at TPulse = 2.5 ms.

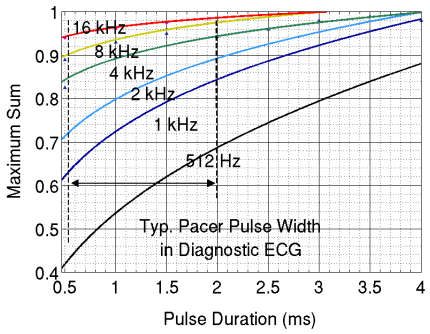

Fig. 8. Max. sum deteriorates with narrow pulse and f_s. Shown at APulse = 5 mV

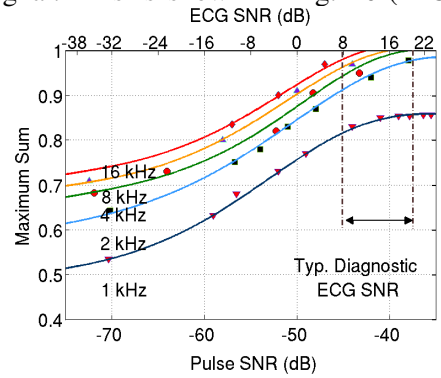

Fig. 9. Max. sum scales with SNR. Shown at APulse (TPulse) = 2 mV (1 ms).

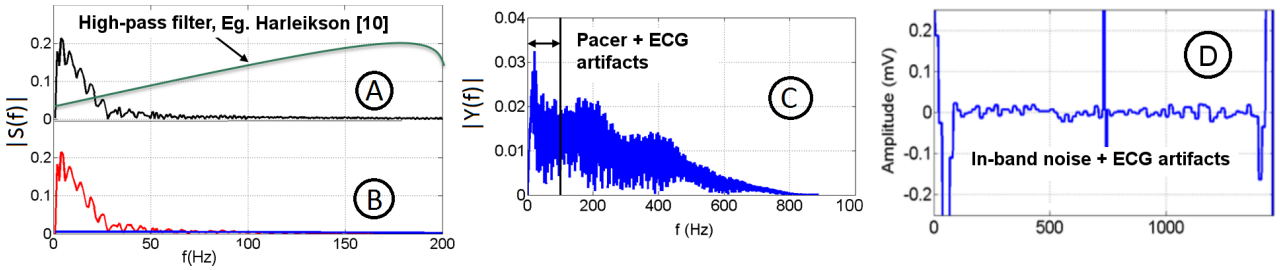

Fig. 10. (A). The differential filter transfer function, $A(f)$, applied to $s[n]$ sampled at 1 kHz (B). The transfer function of $s[n]$ has contributions from $s_{ECG}[n]$, $p[n]$ and $w[n]$ (C). The output, $y[n]$ has reminiscent ECG and noise (D). Time domain signal $y[n]$, shows the pacer-spike with in-band artifacts. The performance degradation of the differential filter detector is mainly due to the co-located ECG artifacts.

The *pacer sub-band*, defined by 50 Hz-1kHz (f_s=2 kHz here) has minimal contribution from the ECG signal. Fig. 10-(D) shows the time domain artifacts, from the two sub-bands, in $y[n]$. The ECG band introduces artifacts whose energy is comparable to the pacer signal which deteriorates the performance of a correlation detector.

The proposed, CS sub-band pacer reconstruction algorithm is shown in Fig. 11. At the sensor node, the input signal $s[n]$ (sparse in the time domain) is transformed to a discrete cosine transform (DCT) sub-space by a transformation Ψ. Here we define a sub-band, f_{sb}, before which we set the DCT coefficients to zero. For example, in the case of Fig. 10-(A), we define f_{sb} = 50 Hz-1 kHz, and set all DCT coefficients in the frequency band 0-50 Hz to zero. This serves as an *ideal, brick-wall, high-pass filter* removing the ECG artifacts in the time domain completely. The output of the filter now has the same transfer function as Fig. 10-(C), except for the 0-50 Hz band where the transform value is set to zero.

Following the ideal, high-pass filtering (of the 0-50 Hz band), we use a measurement matrix *Phi*, in the transform space (f_{sb}), whose dimensions are $M \times f_{sb}$ and each of whose rows contains a single one with a uniform probability in the choice of the column of the non-zero element. We transmit these transform domain samples over the air at an under sampling ratio (USR) of 0.1-0.4. The USR is defined as the ratio of the transmitted samples from the sub-band to the total number of samples in it, *i.e,*. M/f_{sb}. At the processing node which is a data aggregator, such as the PDA in Fig. 1, the compressively sampled sub-band is used to reconstruct the pacer signal alone using the GPSR algorithm. Following this, pacer pulse detection is effectuated by correlation and thresholding like in differential filter based systems.

A. *Performance of the CS sub-band algorithm*

The CS detector filters out time domain ECG artifacts and marginally improves the detection performance of the differential detector. Furthermore, it enables reliable pacer detection using an over-the-air data rate of only about 50-100 sps. Fig. 12 shows the scaling of the pacer detection efficiency versus the SNR. The SNR measurements shown in the figure are made using a 2 mV/2.5 ms, demand-paced, synthetic ECG from ECGsyn and modulated noise models. The CS sub-band, (f_{SB})) varies from 80% to 60% of the sampling frequency, f_s. Fig. 13 shows the scaling of the detection performance as the USR and f_{SB} are varied. The results are shown for Rec#16265 of the MIT-BIH NSRDB. As is seen from the figure, the CS system can enable detection of the EC11 pacer pulses with a diagnostic ECG bandwidth, transmitting only about 10% of the samples over the air to the receiver. The figure shows that a maximum sum of one can be achieved for pacer detection using a sub-band of 50-80% of f_s for pacer reconstruction. Reducing the sub-

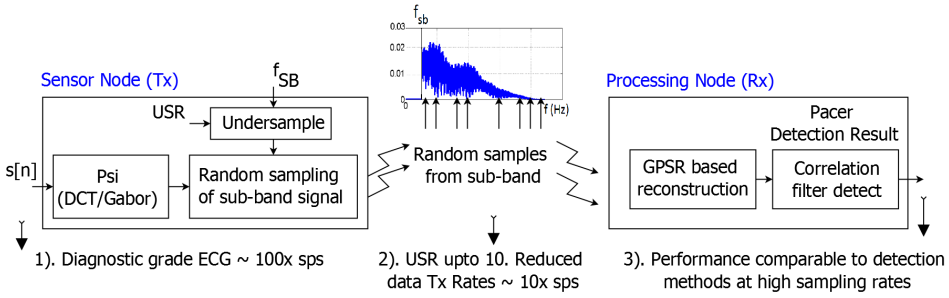

Fig. 11. The CS based sub-band pacer detection algorithm.

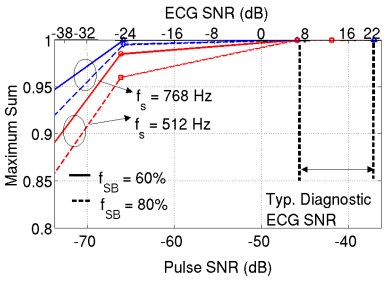

Fig. 12. CS sub-band detection performance vs. SNR at USR = 0.4.

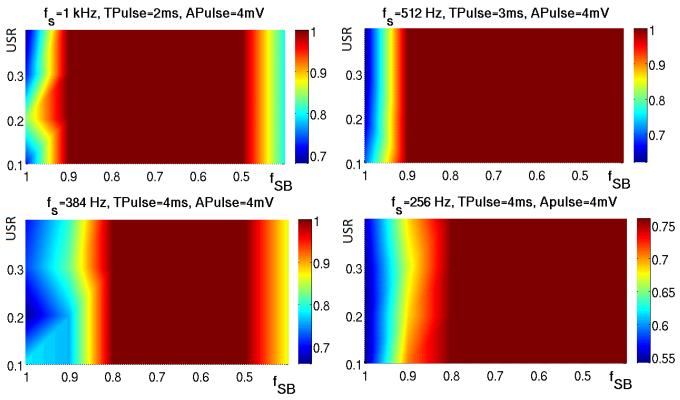

Fig. 13. Pacer detection performance of the CS sub-band algorithm.

band frequency f_{sb} improves the detection performance of the CS algorithm as the contribution from the ECG artifacts is mitigated with decreasing f_{sb}. The figure shows experimental results using diagnostic sampling frequencies, f_s, of 1 kHz, 512 Hz, 384 Hz and 256 Hz. It demonstrates the detection performance of the minimum possible pulse width which can be detected using f_s (i.e., those which result in at least two samples from the pacer signal). For example, the minimum pacer width which can be detected using f_s=1 kHz is 2 ms, which has an energy capture of two samples from the pacer pulse.

V. Conclusions

Detection of pulses from a cardiac pacemaker imposes limitations on the sampling rate of diagnostic grade ECG. For reliable pacer detection, a sampling rate of 4-16 kHz is necessary, which can capture enough energy in the narrow pacer signal. Using patient ECG data from the MIT-BIH NSR database, we demonstrated the limitations on sampling rates using a differential filter based pacer detector. In order to reduce over the air data rates and enable pacer detection in diagnostic bandwidth ECG, we described a compressed sensing based sub-band detection algorithm which can perform pacer detection using an over the air data rate of 50-100 sps.

References

[1] D. Estrin, R. Govindan, J. Heidemann, and S. Kumar, "Next century challenges: Scalable co-ordination in sensor networks," in *Proceedings of the 5th annual ACM/IEEE international conference on Mobile computing and networking*, 1999, pp. 263–270.

[2] A. Mainwaring, D. Culler, J. Polastre, R. Szewczyk, and J. Anderson, "Wireless sensor networks for habitat monitoring," in *Proceedings of the 1st ACM international workshop on Wireless sensor networks and applications*, 2002, pp. 88–97.

[3] E. Jovanov, "Wireless technology and system integration in body area networks for m-health applications," in *IEEE-EMBS 2005. International Conference of the Engineering in Medicine and Biology Society, 2005*, 2006, pp. 7158–7160.

[4] C. Otto, A. Milenkovic, C. Sanders, and E. Jovanov, "System architecture of a wireless body area sensor network for ubiquitous health monitoring," *Journal of Mobile Multimedia*, vol. 1, no. 4, pp. 307–326, Jan 2006.

[5] I. Khalil and F. Sufi, "Real-time ECG data transmission with wavelet packet decomposition over wireless networks," in *Proceedings of the International Conference on Intelligent Sensor Networks and Information Processing (ISSNIP)*, Dec 2008, pp. 267–272.

[6] S. Luo, P. Johnston, and W. Hong, "Performance study of digital pacer spike detection as sampling rate changes," in *Computers in Cardiology, 2008*, 2009, pp. 349–352.

[7] M. Astrom, S. Olmos, and L. Sornmo, "Wavelet based event detection in pacemakers," in *Proceedings of the 23rd Annual International Conference of the IEEE Engineering in Medicine and Biology Society, 2001.*, Nov. 2002, pp. 2121–2124.

[8] M. Jennings, B. Devine, S. Luo, and P. Macfarlane, "Enhanced software based detection of implanted cardiac pacemaker stimuli," in *Computers in Cardiology, 2009*, 2010, pp. 833–836.

[9] E. Herleikson, "ECG pace pulse detection and processing," Nov. 1997, US Patent 5,682,902.

[10] E. Helfenbein, J. Lindauer, S. Zhou, R. Gregg, and E. Herleikson, "A software-based pacemaker pulse detection and paced rhythm classification algorithm," *Journal of electrocardiology*, vol. 35, no. 4, pp. 95–103, 2002.

[11] A. Polpetta and P. Banelli, "Fully digital pacemaker detection in ECG signals using a non-linear filtering approach," in *EMBS 2008. 30th Annual International Conference of the IEEE Engineering in Medicine and Biology Society, 2008.*, 2008, pp. 5406–5410.

[12] P. Banelli and A. Polpetta, "System for detecting pacing pulses in electrocardiogram signals," Feb. 2010, WO Patent WO/2010/018,608.

[13] H. Garudadri, P. Baheti, S. Majumdar, C. Lauer, F. Mass and, J. van de Molengraft, and J. Penders, "Artifacts mitigation in ambulatory ecg telemetry," in *12th IEEE International Conference on e-Health Networking Applications and Services (Healthcom), 2010*, 2009, pp. 338–344.

[14] G. Moody, R. Mark, and A. Goldberger, "PhysioNet: a Web-based resource for the study of physiologic signals," *IEEE Engineering in Medicine and Biology Magazine*, vol. 20, no. 3, pp. 70–75, 2002.

[15] ANSI/AAMI EC11, "Diagnostic electrocardiographic devices, ANSI/AAMI standard," Jan. 2007.

[16] M. A. T. Figueiredo, R. D. Nowak, and S. J. Wright, "Gradient projection for sparse reconstruction: Application to compressed sensing and other inverse problems," *IEEE Journal of Selected Topics in Signal Processing*, vol. 1, no. 4, pp. 586–597, 2008.

[17] J. Haupt, W. Bajwa, M. Rabbat, and R. Nowak, "Compressed sensing for networked data," *IEEE Signal Processing Magazine*, vol. 25, no. 2, pp. 92–101, 2008.

[18] E. Candes and T. Tao, "Near-optimal signal recovery from random projections: Universal encoding strategies," *IEEE Transactions on Information Theory*, vol. 52, no. 12, pp. 5406–5425, 2006.

[19] D. Donoho, "Compressed sensing," *IEEE Transactions on Information Theory*, vol. 52, no. 4, pp. 1289–1306, 2006.

[20] P. McSharry, G. Clifford, L. Tarassenko, and L. Smith, "A dynamical model for generating synthetic electrocardiogram signals," *IEEE Transactions on Biomedical Engineering*, vol. 50, no. 3, pp. 289–294, 2003.